Fibrillin degradation by matrix metalloproteinases: implications for connective tissue remodelling

Jane L. ASHWORTH*, Gillian MURPHY†, Matthew J. ROCK*, Michael J. SHERRATT*, Stephen D. SHAPIRO‡, C. Adrian SHUTTLEWORTH* and Cay M. KIELTY*[1]

*Wellcome Trust Centre for Cell-Matrix Research, School of Biological Sciences, University of Manchester, 2.205 Stopford Building, Oxford Road, Manchester M13 9PT, U.K., †School of Biological Sciences, University of East Anglia, Norwich NR4 7TJ, U.K., and ‡Departments of Medicine and Cell Biology and Physiology, Washington University School of Medicine at Barnes-Jewish Hospital, St. Louis, MO 63110, U.S.A.

Fibrillin is the principal structural component of the 10–12 nm diameter elastic microfibrils of the extracellular matrix. We have previously shown that both fibrillin molecules and assembled microfibrils are susceptible to degradation by serine proteases. In this study, we have investigated the potential catabolic effects of six matrix metalloproteinases (MMP-2, MMP-3, MMP-9, MMP-12, MMP-13 and MMP-14) on fibrillin molecules and on intact fibrillin-rich microfibrils isolated from ciliary zonules. Using newly synthesized recombinant fibrillin molecules, major cleavage sites within fibrillin-1 were identified. In particular, the six different MMPs generated a major degradation product of ~ 45 kDa from the N-terminal region of the molecule, whereas treatment of truncated, unprocessed and furin-processed C-termini also generated large degradation products. Introduction of a single ectopia lentis-causing amino acid substitution (E2447K; one-letter symbols for amino acids) in a calcium-binding epidermal growth factor-like domain, predicted to disrupt calcium binding, markedly altered the pattern of C-terminal fibrillin-1 degradation. However, the fragmentation pattern of a mutant fibrillin-1 with a comparable E → K substitution in an upstream calcium-binding epidermal growth factor-like domain was indistinguishable from wild-type molecules. Ultrastructural examination highlighted that fibrillin-rich microfibrils isolated from ciliary zonules were grossly disrupted by MMPs. This is the first demonstration that fibrillin molecules and fibrillin-rich microfibrils are degraded by MMPs and that certain amino acid substitutions change the fragmentation patterns. These studies have important implications for physiological and pathological fibrillin catabolism and for loss of connective tissue elasticity in ageing and disease.

Key words: catabolism, microfibrils, mutations.

INTRODUCTION

The fibrillin-rich microfibrils endow tissues with long-range elastic recoil and, in evolutionary terms, may be the most fundamental elastic components of extracellular matrix [1–4]. They form the template for tropoelastin deposition during elastic fibrillogenesis and in mature elastic fibres a microfibrillar mantle surrounds a central core of cross-linked elastin [5]. Isolated microfibrils have a complex architecture with pronounced beads connected by inter-bead filaments, with a diameter of 10–12 nm and average axial periodicity of ~ 56 nm [2,6,7]. Overwhelming evidence now exists that polymerized fibrillin molecules form the structural fibrillar framework of microfibrils. Purification, monoclonal antibody production and detailed immunolocalization studies have all identified fibrillins as the major structural elements of this class of microfibrils [6–11]. Moreover, mutations in the two fibrillin genes cause Marfan syndrome and related heritable connective tissue diseases which are associated with microfibrillar deficiencies [12].

The two fibrillin isoforms are large glycoproteins (~ 350 kDa) with a complex multidomain structure, including 47 epidermal growth factor (EGF)-like domains, 43 of which have calcium-binding consensus sequences (cbEGF-like domains) [13,14]. Calcium binding has been shown to have a major influence on the organization of fibrillin molecules and fibrillin-rich microfibrils [15,16]. The proline-rich region towards the N-terminus is predicted to act as a 'hinge-like' region within the molecule. C-terminal processing at a tetrabasic furin cleavage site influences the deposition of microfibrillar networks [17] and may regulate polymerization of newly secreted fibrillin in the extracellular space. Several other molecules colocalize with microfibrils, but it is not known whether they contribute structurally to microfibrils. They include microfibril-associated glycoprotein-1, which associates with beads and may mediate interactions with tropoelastin [18], latent transforming growth factor-β binding proteins (LTBPs) [19] and fibulin-2 [20].

Ultrastructural studies indicate that microfibril assembly is a pericellular event, but neither how fibrillin molecules assemble nor their molecular arrangement within microfibrils has been clearly defined. One model, based on antibody epitope mapping and measured molecular dimensions, suggests a parallel head-to-tail alignment of unstaggered fibrillin monomers with N- and C-termini at, or close to, the beads [21]. Staggered arrangements based on extrapolation of molecular length from cbEGF-like domain dimensions, or on alignment of transglutaminase cross-link sites, have also been proposed [22,23]. N- and C-terminal interactions are thought to drive assembly and, in a mouse model, fibrillin-1 molecules with intact terminal sequences but a central deletion were able to assemble fibrillin-1-based microfibrils [11].

In ageing and in diseases such as pulmonary emphysema and atherosclerosis, damage to elastic fibres is often apparent ultrastructurally as progressive loss of the microfibrillar mantle and erosion of the elastin core and, functionally, as impaired tissue

Abbreviations used: cb, calcium-binding consensus sequence; EGF, epidermal growth factor; EM, electron microscopy; LTBP, latent transforming growth factor-β binding protein; STEM, scanning transmission electron microscopy.

[1] To whom correspondence should be addressed (e-mail cay.kielty@man.ac.uk).

extensibility [24–26]. Fibrillin-1 mutations cause reduced or disordered microfibril deposition in Marfan skin fibroblast cultures and abnormal elastic fibres are also a characteristic feature of Marfan syndrome, resulting in shortened life expectancy due to aortic dissection [12,27]. Disease-causing fibrillin-1 mutations are distributed throughout the coding region of the molecule, including N- and C-terminal sequences, and many of these result in amino acid substitutions within cbEGF-like domains which are predicted to disrupt calcium binding and/or domain conformation. Other mutations include exon deletions and premature terminations. Microfibrillar deficiencies contribute to other heritable connective tissue conditions, including mitral valve prolapse syndrome and aortic aneurysms.

Progressive destruction of fibrillin-rich microfibrils by a battery of pericellular matrix-degrading proteinases secreted by resident cells and by inflammatory cells that infiltrate tissues may contribute to loss of elastic fibre function in ageing and inflammatory disease. The matrix metalloproteinases (MMPs) constitute a large family of structurally related matrix-degrading proteinases which may be secreted by mesenchymal cells, macrophages and polymorphonuclear leukocytes [28,29]. They include interstitial collagenases (MMP-1, MMP-8, MMP-13), stromelysins (MMP-3, MMP-10), 72 kDa and 92 kDa gelatinases (MMP-2, MMP-9), matrilysin (MMP-7), macrophage metalloelastase (MMP-12) and membrane-type MMPs (MMP-14, MMP-15, MMP-16, MMP-17). A number of these MMPs possess elastinolytic activity and are thus implicated in elastin and elastic fibre turnover; they include MMP-2, MMP-3, MMP-7, MMP-9, MMP-12 and MMP-13 [29]. MMPs and their inhibitors have been described in the aqueous cavity of the eye [30–34] and also in the vitreous cavity, where they may contribute to normal and pathological remodelling. The proteolytic capacity of MMPs is normally tightly controlled at the transcriptional level and post-translationally by regulated activation and naturally occurring inhibitors. Their excessive or inappropriate expression and activation may contribute to the development of life-threatening diseases associated with loss of connective tissue elasticity.

We have previously demonstrated that enzymes of the serine proteinase class secreted by inflammatory cells effectively degrade both fibrillin molecules and assembled microfibrils [35]. However, the potential destructive effect of MMPs on these crucial connective tissue molecules and microfibrils has not been documented. In this study, we have investigated whether six different MMPs are able to degrade recombinant fibrillin molecules and isolated assembled fibrillin-rich microfibrils. Since fibrillins are large molecules that have to date proved difficult to express as full-length molecules, we focussed on the N- and C-terminal regions which make a crucial contribution to the assembly and integrity of microfibrils. We were particularly interested in investigating whether the unusual proline-rich region might be a proteolytically susceptible sequence. In a related molecule, LTBP-1, a proline-rich linker region undergoes proteolysis with removal of the N-terminus and release from matrix storage sites [19]. We also examined the consequences for MMP susceptibility of introducing a disease-causing (E2447K) amino acid substitution (one-letter code for amino acids) within a cbEGF-like domain (exon 59) and a similar E → K mutation in an upstream cbEGF-like domain (exon 53).

MATERIALS AND METHODS

Materials

MMP-2, MMP-3, MMP-9, MMP-13 and MMP-14 were purified as previously described [36–39]. Murine and human MMP-12 (murine metalloelastase; human metalloelastase) were prepared as recombinant catalytic domains (22 kDa) as previously described [40].

Human cDNA clones encoding full-length fibrillin-1 were supplied by Dr F. Ramirez (Mt. Sinai School of Medicine, New York, NY, U.S.A.) [14].

Fibrillin-1 cDNAs

Six fibrillin cDNAs were constructed in order to generate mRNAs for translation and digestion studies (Figure 1). All constructs were verified by automated dye-terminator sequencing.

(1) A fibrillin-1 C-terminal cDNA clone (cFib-1) encoding exons 50–65 was constructed from clone F3.4 [14]. Three mutant forms of cFib-1 were also created by site-directed mutagenesis (QuikChange Site-Directed Mutagenesis Kit, Stratagene Ltd., Cambridge, U.K.) (Figure 1). A G → A point mutation in exon 59 resulted in a glutamic acid to lysine amino acid substitution (E2447K) in an cbEGF-like domain; this mutant molecule was designated cFib-1^{E2447K}. This amino acid substitution was previously identified in a family with dominant ectopia lentis [41]. A glutamic acid to lysine substitution (E2169K) was introduced into a cbEGF-like domain encoded by exon 52 (cFib-1^{E2169K}).

(2) A shortened form of cFib-1 (scFib-1) encoding exons 48–63 was constructed from clone F3.4 [14].

(3) A fibrillin-1 N-terminal cDNA clone (nFib-1) encoding exons 1–15 was constructed from clone 5′F [14].

(4) A truncated nFib-1 (snFib-1) encoding exons 1–8 was constructed from nFib-1.

(5) A fibrillin-1 cDNA clone (proFib-1) encoding exons 9–11 was constructed by reverse transcriptase PCR using human dermal fibroblast mRNA.

(6) A fibrillin-2 cDNA clone (glyFib-2) encoding exons 9–11, including the glycine-rich region, was constructed by reverse transcriptase PCR using human keratinocyte mRNA.

Transcription of fibrillin-1 cDNAs

Fibrillin-1 cDNAs were subcloned into vector pSecTagA (Invitrogen) at *Eco*R1 sites and linearized with *Pme*1 (New England Biolabs). DNA was purified by phenol/chloroform extraction. Transcription was performed using T7 RNA polymerase at 37 °C for 3 h followed by column RNA purification (Qiagen) and elution in 50 μl of RNase-free water with 1 mM dithiothreitol and 40 units of RNase inhibitor added. Newly generated RNA was heated to 60 °C for 10 min before use to disrupt secondary structure.

Preparation of semi-permeabilized HT1080 cells

Semi-permeabilized HT1080 cells were prepared as previously described [42–45]. This system has been shown effectively to recapitulate folding and post-translational modifications of newly translated proteins destined for the extracellular matrix. Briefly, a 75 cm^2 flask of cells was grown to confluency, treated with trypsin and resuspended in 8 ml of 20 mM Hepes, pH 7.2, containing 10 mM potassium acetate, 2 mM magnesium acetate and 100 μg/ml soybean trypsin inhibitor (KHM buffer), then pelleted at 10000 ***g*** for 3 min. Cells were resuspended in 6 ml of KHM buffer containing 40 μg/ml digitonin and incubated on ice for 5 min. KHM (8 ml) was added to terminate permeabilization, then the cells were pelleted and resuspended in 11 ml of 50 mM Hepes, pH 7.2/90 mM potassium acetate. After 10 min, the cells were pelleted and resuspended in 100 μl of KHM. Staphylococcal nuclease (10 μg/ml) and calcium chloride to a final concentration of 1 mM were added, and the cells were incubated at room

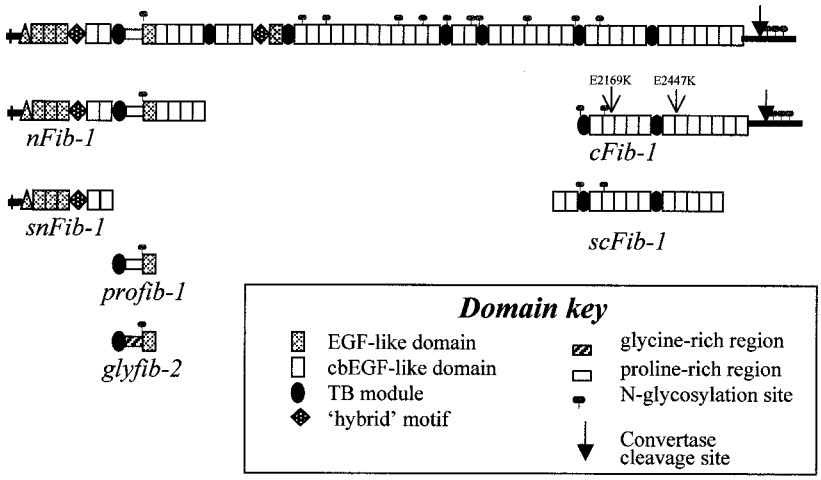

Figure 1 Fibrillin-1 constructs

Human fibrillin cDNAs were prepared that encoded the recombinant proteins utilized in this study (see the Materials and methods section). They were cFib-1, the C-terminal region of fibrillin-1; scFib-1, a shortened form of cFib-1; nFib-1, an N-terminal region of fibrillin-1; snFib-1, a shortened form of nFib-1; proFib-1, a three-domain peptide comprising the proline-rich region of fibrillin-1 and flanking domains; glyFib-2, a three-domain peptide comprising the glycine-rich region of fibrillin-2 and flanking domains. The convertase cleavage site close to the C-terminus and positions of amino acid substitutions are indicated by arrows. The triangular symbol denotes a novel N-terminal cysteine-rich sequence.

temperature for 12 min. The reaction was terminated by adding EGTA to a final concentration of 4 mM and the cells were pelleted and resuspended in 100 μl of KHM.

In vitro translation in the presence of semi-permeabilized cells

Fibrillin-1 RNA was translated in the presence of semi-permeabilized HT1080 cells using a rabbit reticulocyte lysate (Flexilysate, Promega, Southampton, U.K.) for 1.5 h at 30 °C. Each reaction contained 35 μl of lysate, 1 μl of RNase inhibitor, 1 μl of amino acids minus methionine or cysteine, 1 μl of potassium chloride, 2.5 μl of [^{35}S]methionine (15 μCi) or 3 μl of [^{35}S]cysteine (10 μCi/μl) and 2.5 μl of prepared RNA. In all cases, fibrillin was the only labelled translated protein generated.

Proteinase K digestions (250 μg/ml) were carried out as previously reported, with or without 1% Triton X-100 to lyse intracellular organelles, to confirm that newly translated fibrillin-1 had been translocated [42–45]. Each mixture was incubated on ice for 10 min, then the reaction was stopped by addition of PMSF to a concentration of 10 mM and incubation on ice for 5 min.

Endoglycosidase H treatment was used to confirm that translocated fibrillin-1 had been N-glycosylated within the endoplasmic reticulum. The cells were pelleted and resuspended in 40 μl of endoglycosidase H buffer [0.1 M Tris/HCl, pH 8.0/1% (v/v) SDS/1% (v/v) 2-mercaptoethanol] and boiled for 5 min. Samples were centrifuged for 5 min at 13000 ***g*** to remove insoluble material and the supernatant was mixed with 40 μl of sodium citrate, pH 5.5. The sample was split into two and 1 m-unit of endoglycosidase H was added to one of the aliquots. Both aliquots were incubated at 37 °C for 18 h, then SDS/PAGE loading buffer with dithiothreitol to 50 mM was added before SDS/PAGE analysis and autoradiography.

Enzyme incubations with fibrillin molecules

^{35}S-Labelled recombinant fibrillin-1 molecules generated using the cell-free translation system supplemented with semi-permeabilized HT1080 cells were equilibrated in 10 mM Tris/HCl, pH 7.4, containing 200 mM NaCl and 10 mM $CaCl_2$ and used as substrates in MMP incubations.

ProMMP-2 (259 μg/ml) was activated by pre-treatment with 1 mM 4-aminophenylmercuric acetate for 1 h at 25 °C. ProMMP-9 (290 μg/ml) was activated by pre-treatment with 1 mM 4-aminophenylmercuric acetate for 1.5 h at 37 °C. ProMMP-3 (240 μg/ml) was activated by addition of trypsin (10 μg/ml) at 37 °C for 20 min; this activation step was effectively terminated by addition of excess of soybean trypsin inhibitor (1 mg/ml). MMP-12 (275 μg/ml), MMP-13 (80 μg/ml) and MMP-14 (78 μg/ml) did not require activation.

For most experiments, each enzyme was incubated for up to 18 h at 37 °C with the recombinant protein samples. Final enzyme concentrations were 25.9 μg/ml for MMP-2, 24 μg/ml for MMP-3, 29 μg/ml for MMP-9, 27.5 μg/ml for MMP-12, 8 μg/ml for MMP-13 and 7.8 μg/ml for MMP-14. Enzyme incubations, and controls with no added enzyme, were analysed by SDS/PAGE on 6%, 8% or 15% gels under reducing conditions and visualized by autoradiography. The prestained molecular-mass markers used were myosin (250 kDa), phosphorylase B (148 kDa), glutamate dehydrogenase (60 kDa), carbonic anhydrase (42 kDa), myoglobin (red, 30 kDa), myoglobin (blue, 22 kDa) and lysozyme (17 kDa) (Novex, Inc., San Diego, CA, U.S.A.). In some experiments, the following prestained SDS/PAGE markers were used: β-galactosidase (126 kDa), BSA (89 kDa), ovalbumin (89 kDa), soybean trypsin inhibitor (28.4 kDa) (Bio-Rad). The positions of molecular-mass markers are indicated on the left of the gels.

Isolation of intact microfibrils

Intact fibrillin-rich microfibrils were isolated from human zonular filaments in the presence of freshly prepared protease inhibitors (2 mM PMSF/5 mM *N*-ethylmaleimide), as previously described [46,47]. The zonular filaments were obtained from individuals of 38, 48 and 68 years of age from the Corneal Transplant Service Eye Bank, Manchester. Size fractionation on a Sepharose CL-2B column yielded an excluded volume (V_0) that contained abundant extensive fibrillin-rich microfibrils (1.5–2.0 mg/ml).

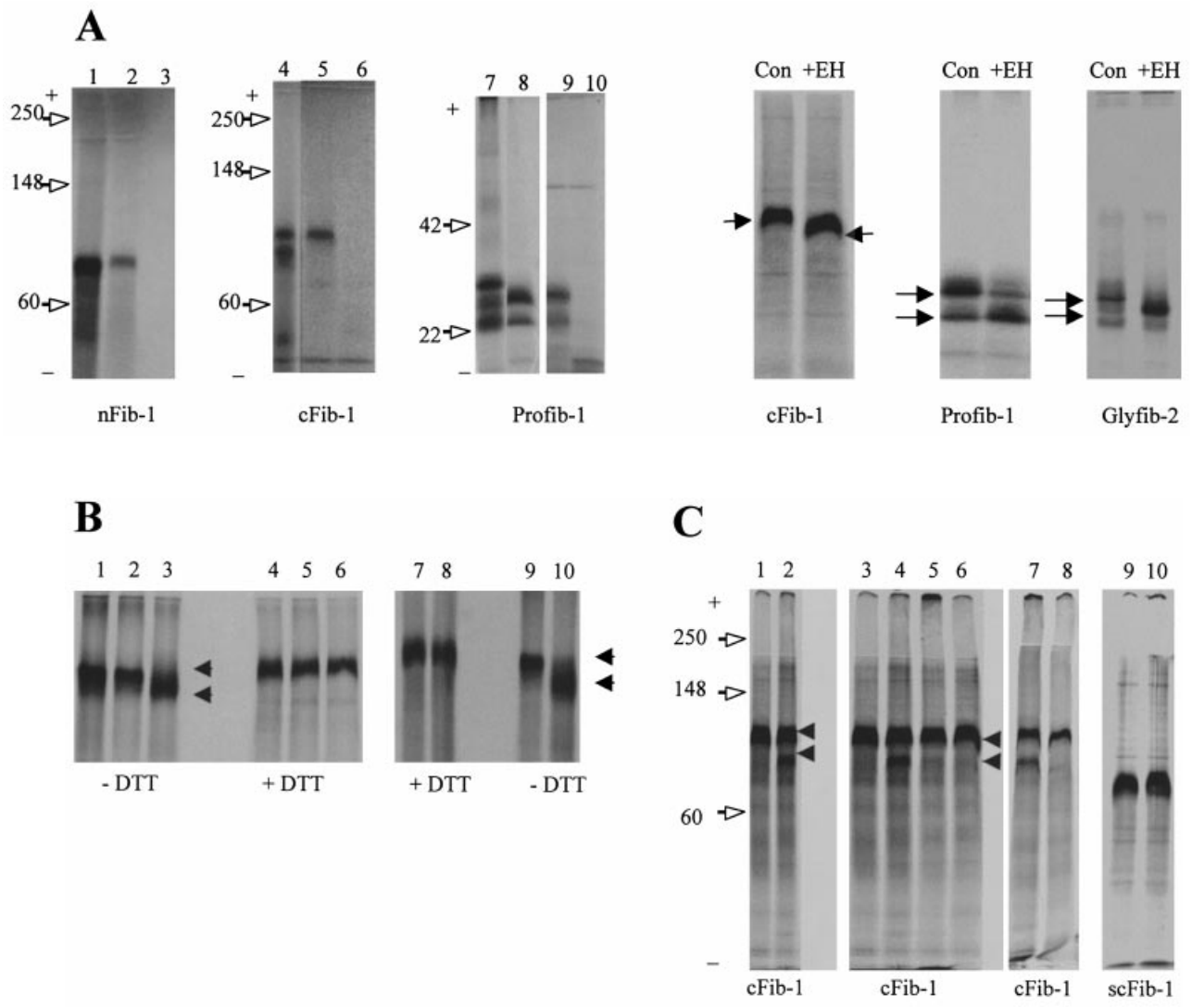

Figure 2 Electrophoretic analysis of newly synthesized recombinant fibrillin molecules

^{35}S-Labelled fibrillin molecules were generated using a cell-free translation system supplemented with semi-permeabilized HT1080 cells [42–45]. Samples were run on 8% SDS/PAGE gels (nFib-1 and cFib-1) or 15% SDS/PAGE gels (proFib-1 and glyFib-2). All samples were run in the presence of dithiothreitol, except proFib-1 (lane 7). (**A**) Translocation of newly-translated fibrillin molecules. Lanes 1-3, nFib-1; lanes 4–6, cFib-1; lanes 7–10, proFib-1; lanes 1, 4 and 9, cell-free translation mixture plus semi-permeabilized cells; lanes 2, 5 and 10, cell-free translation mixture plus semi-permeabilized cells after proteinase K digestion; lanes 3 and 6, cell-free translation mixture plus semi-permeabilized cells after treatment with Triton X-100 in the presence of proteinase K. Translocated protein was protected from proteinase K degradation unless pre-treated with Triton X-100. nFib-1 (results not shown), cFib-1, proFib-1 and glyFib-2 were also treated with endoglycosidase H (EH) before SDS/PAGE analysis. This treatment removed N-linked carbohydrate in all cases and resulted in faster electrophoretic migration. Con, control. (**B**) Effects of reduction and calcium on electrophoretic migration of cFib-1. Under non-reducing conditions cFib-1 migrated slightly faster than after reduction. Under non-reducing conditions after treatment with EGTA cFib-1 migrated faster than in the presence of calcium. No calcium or EGTA effects were apparent after reduction. The cFib-1^{E2447K} mutation is predicted to disrupt calcium binding. cFib-1^{E2447K} exhibited faster migration than wild-type cFib-1 under non-reducing conditions. Wild-type cFib-1, lanes 1–6, 7 and 9. Mutant cFib-1^{E2447K}, lanes 8 and 10. Lanes 1 and 4, no added $CaCl_2$ or EGTA; lanes 2 and 5, +10 mM $CaCl_2$; lanes 3 and 6, +10 mM EGTA; lanes 7–10, no added $CaCl_2$ or EGTA. (**C**) C-terminal processing of cFib-1. Lanes 1–8, cFib-1; lanes 9 and 10, scFib-1. Incubation of washed cell lysates at 4 °C, lanes 1, 3 and 9. Incubation of washed cell lysates at 37 °C, lanes 2, 4–8 and 10. When washed cell lysates were incubated at 4 °C no processing was observed. However, when washed lysed cells were incubated at 37 °C for 18 h processing of cFib-1 with loss of ~ 20 kDa occurred. Under these conditions scFib-1 protein did not undergo cleavage, confirming that processing was at the C-terminus of fibrillin-1. Processing was due to furin-like proteolytic activity since PMSF (lane 5), EGTA (lane 6) and decanoyl-RKVR-chloromethylketone (lane 8) all inhibited processing.

Enzyme incubations with fibrillin-rich microfibrils

Intact fibrillin-rich microfibrils were equilibrated in 10 mM Tris/HCl, pH 7.4, containing 200 mM NaCl and 10 mM $CaCl_2$ and then incubated for 18 h at 37 °C with or without added MMPs. For each incubation 50 μl of V_o fraction was used. Final enzyme concentrations in these incubations were (a) MMP-2 (10.4 μg/ml), MMP-3 (9.6 μg/ml), MMP-9 (11.6 μg/ml), MMP-12 (11.0 μg/ml), MMP-13 (3.2 μg/ml) and MMP-14 (3.1 μg/ml) or (b) MMP-2 (27.5 μg/ml), MMP-3 (24.0 μg/ml), MMP-9 (29.0 μg/ml), MMP-12 (27.5 μg/ml), MMP-13 (8.0 μg/ml) and MMP-14 (7.8 μg/ml).

Ultrastructural analysis of microfibrils

Electron microscopy (EM) studies were conducted to investigate the potential catabolic effects of the MMPs. Dark field scanning transmission electron microscopy (STEM) of unstained, un-

shadowed control and enzyme-treated microfibril preparations were carried out as previously described [48]. This approach provided quantitative data on microfibril length and periodicity. Rotary shadowing EM was used to visualize ultrastructural changes in the MMP-treated microfibrils [2,16].

RESULTS

Recombinant fibrillin molecules

The predicted molecular masses of the fibrillin molecules encoded by the cDNA constructs before N-glycosylation are as follows: cFib-1, 90 kDa; scFib-1, 65 kDa; nFib-1, 68 kDa; snFib-1, 35 kDa; proFib-1, 18 kDa; glyFib-2, 18 kDa (Figure 1). All of these molecules, except snFib-1, contained one or more N-glycosylation sites. Labelled recombinant protein was produced using a cell-free translation system supplemented with semi-permeabilized HT1080 cells (Figures 2–4). This system has been shown effectively to recapitulate folding and post-translational modifications of matrix molecules [42–45].

In all cases, newly-synthesized fibrillin-1 was translocated into the endoplasmic reticulum where it was protected from proteinase K digestion, except after Triton X-100 treatment (Figure 2A). Endoglycosidase H removed N-linked carbohydrate from nFib-1, proFib-1, glyFib-2 and cFib-1 as judged by faster electro-

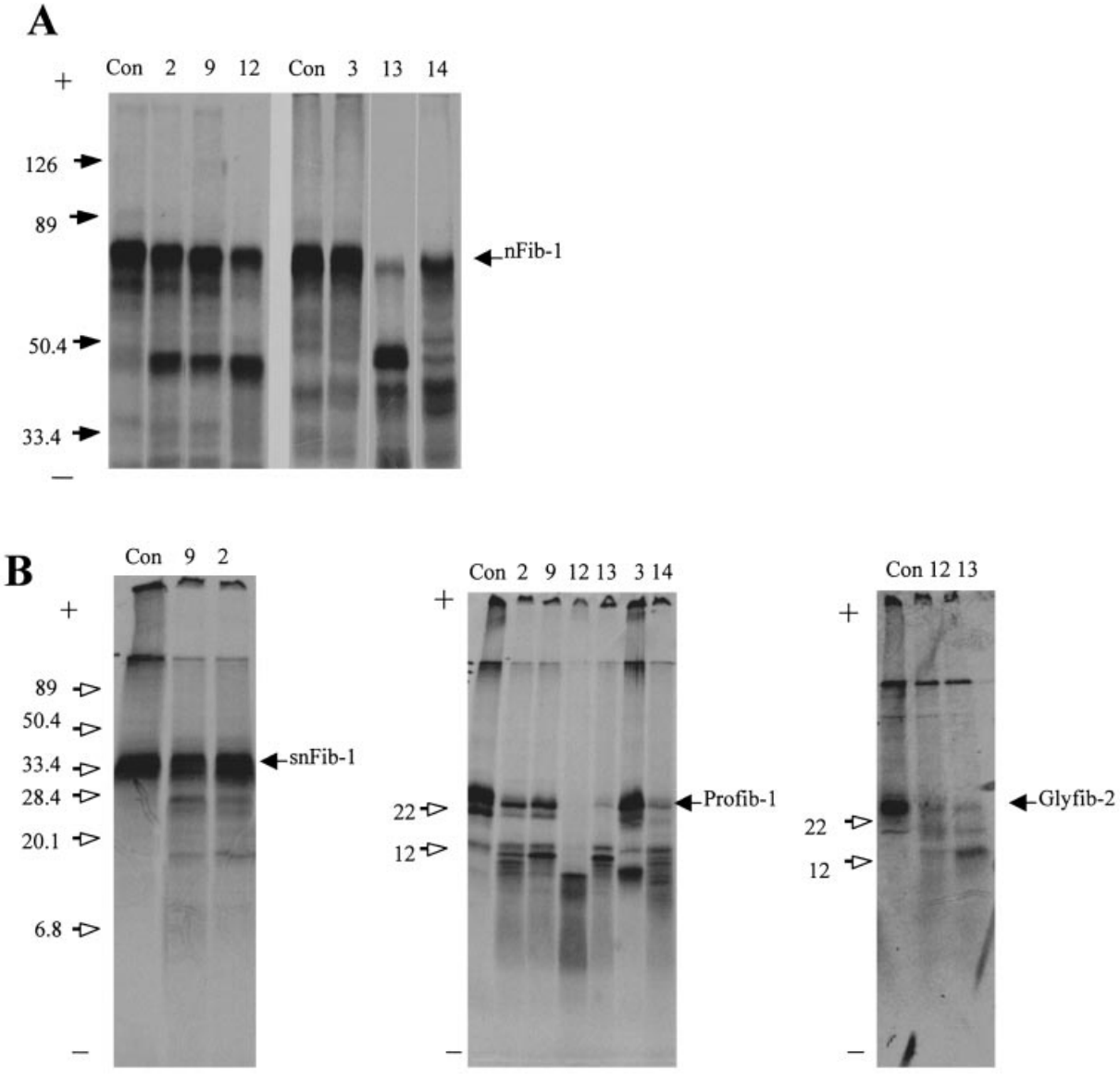

Figure 3 Electrophoretic analysis of MMP-treated recombinant N-terminal fibrillin

MMP digestions were carried out on ^{35}S-labelled newly-synthesized recombinant nFib-1 and the three-domain peptides as described in the Materials and methods section. The final concentrations of each MMP used were 25.9 μg/ml for MMP-2, 24 μg/ml for MMP-3, 29 μg/ml for MMP-9, 27.5 μg/ml for MMP-12, 8 μg/ml for MMP-13 and 7.8 μg/ml for MMP-14. Samples were run on 8% SDS/PAGE gels (nFib-1) or 15% SDS/PAGE gels (proFib-1 and glyFib-2) under reducing conditions. The numbers above the lanes indicate the MMP used in each case. Con, control. (**A**) nFib-1 was digested for 2 h with MMP-2, MMP-3, MMP-9, MMP-12, MMP-13 and MMP-14. A major degradation product of $\sim$ 45 kDa was generated after digestion with MMP-2, MMP-9, MMP-12 and MMP-13. MMP-14 degraded nFib-1 to several fragments. (**B**) snFib-1 was treated with MMP-2 and MMP-9 for 2 h and several minor fragments but no major products were apparent. When proFib-1 was digested for 2 h with the MMPs all six enzymes were shown to cleave proFib-1, generating prominent $\sim$ 9–12 kDa products. Glyfib-2 was also cleaved by MMP-12 and MMP-13 to similar-sized products.

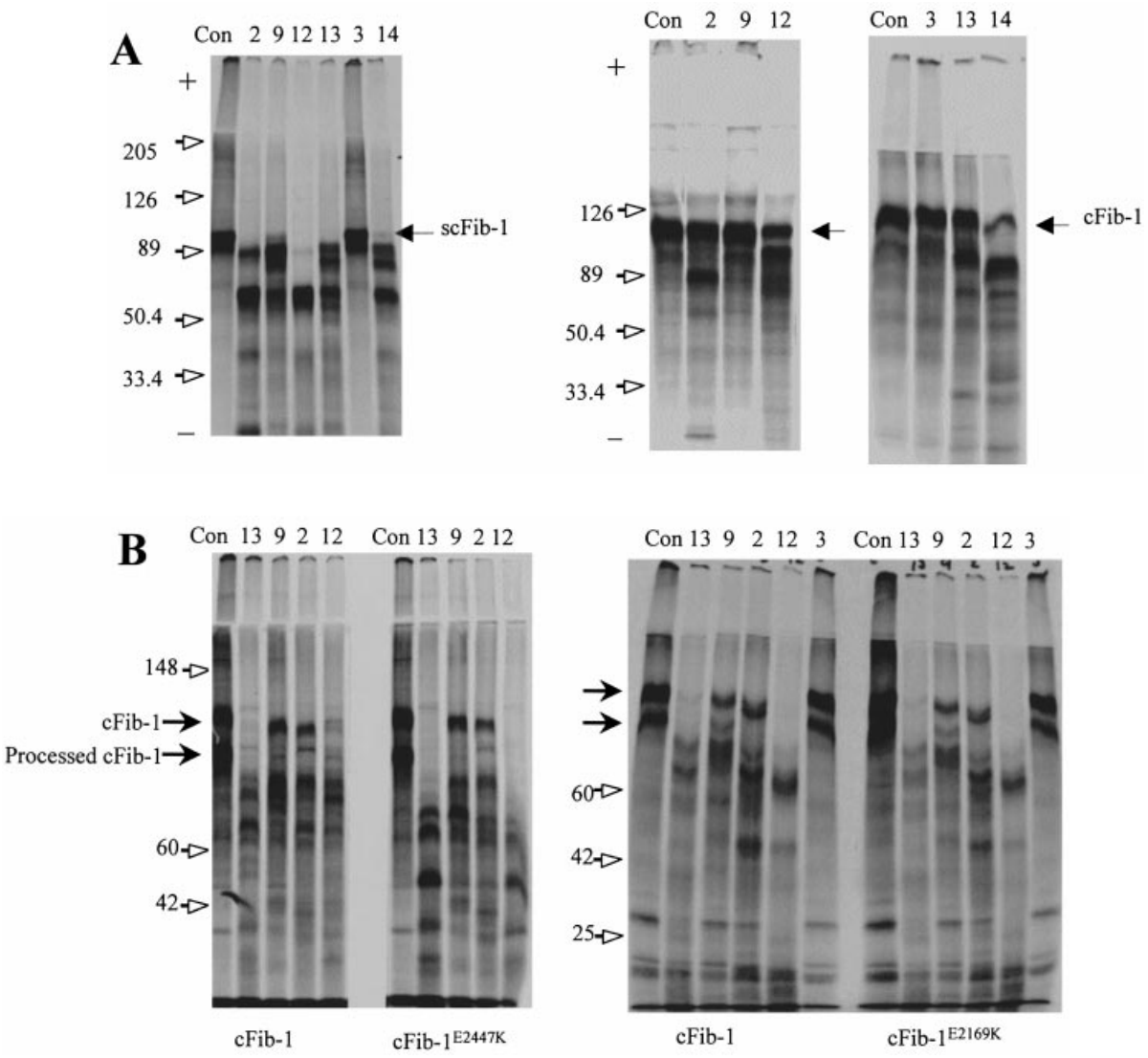

Figure 4 Electrophoretic analysis of MMP-treated recombinant C-terminal fibrillin

MMP digestions were carried out on ^{35}S-labelled newly synthesized recombinant cFib-1 and scFib-1 as described in the Materials and methods section. The final concentration of each MMP used were in each case 25.9 μg/ml for MMP-2, 24 μg/ml for MMP-3, 29 μg/ml for MMP-9, 27.5 μg/ml for MMP-12, 8 μg/ml for MMP-13 and 7.8 μg/ml for MMP-14. Samples were run on 8% SDS/PAGE gels under reducing conditions. The numbers above the lanes indicate the MMP used in each case. Con, control. (**A**) cFib-1 was digested for 2 h with each MMP. Major degradation products of $\sim$ 89–95 kDa were generated after digestion with MMP-2, MMP-9, MMP-12, MMP-13 and MMP-14. scFib-1 generated a major $\sim$ 65 kDa fragment after incubation with all enzymes except MMP-3, indicating a major cleavage site within this sequence. (**B**) Both unprocessed and processed cFib-1 were effectively cleaved by the MMPs. Fragments of $\sim$ 20–25 kDa may represent processed C-terminal fragments. Comparison of the fragmentation patterns of wild-type cFib-1 and the exon 59 mutant molecule cFib-1^{E2447K} revealed that this mutant had an altered degradation-product profile. In particular, a major novel $\sim$ 47 kDa fragment was apparent after MMP-13 and MMP-12 digestions. In marked contrast, the cFib-1^{E2169K} mutant molecules had fragmentation profiles indistinguishable from wild-type molecules.

phoretic migration (Figure 2A). Translocated proteins were able to bind calcium since under non-reducing conditions electrophoretic mobility was altered following incubation with EGTA or calcium (Figure 2B). All subsequent experiments utilized the translocated labelled fibrillin-1 molecules released from rigorously washed and lysed cells and were carried out in the presence of 10 mM calcium.

When washed, lysed cells were boiled in gel sample buffer and electrophoresed directly or incubated at 4 °C, no processing of cFib-1 was detected. However, when washed and lysed cells were incubated at 37 °C for 2–18 h, cFib-1 underwent a specific cleavage event with loss of $\sim$ 20 kDa (Figure 2C). Processing was not seen when cell lysates containing a shortened form of cFib-1 (scFib-1) were incubated at 37 °C. Processing was inhibited by decanoyl-RVKR-chloromethyl ketone (13.4 mM), a selective synthetic furin inhibitor [49], and by PMSF (2 mM) and EGTA (40 mM). No furin processing of nFib-1 (predicted to remove $\sim$ 2 kDa) was discerned electrophoretically.

Digestion of N-terminal recombinant fibrillin-1 molecules

Labelled recombinant nFib-1 was incubated with the six MMPs for 15 min, 2 h and 20 h to investigate whether these enzymes cleaved this N-terminal region of fibrillin-1. Incubation with MMP-2, MMP-9, MMP-12 and MMP-13 for 2 h generated a major degradation product of $\sim$ 45 kDa (Figure 3A). By 20 h,

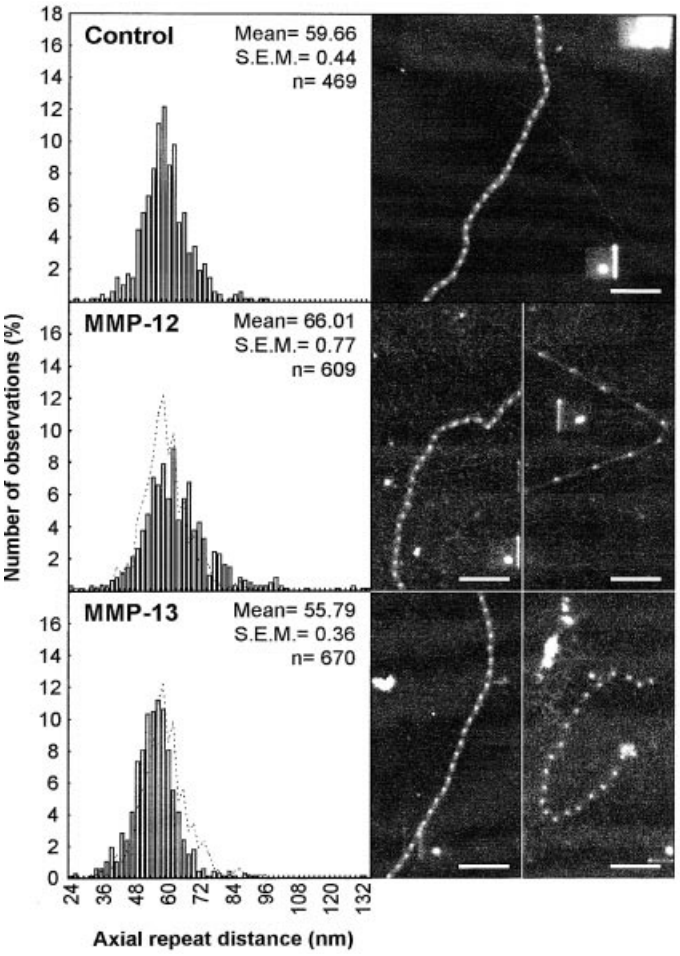

Figure 5 Periodicity of MMP-treated microfibrils from a 48-year-old individual, determined by dark-field STEM

After treatment with MMP-12 (final concentration 11.0 μg/ml) or MMP-13 (final concentration 3.2 μg/ml) many long microfibrils were apparent which often contained areas of extended periodicity. Mean microfibril periodicity increased significantly after treatment with MMP-12 (analysis of variance, $P < 0.001$). Longer incubations or increased enzyme concentration (MMP-12, 27.5 μg/ml; MMP-13, 8 μg/ml) resulted in extensive microfibril destruction. The dotted line represents the control profile. Scale bar = 200 nm.

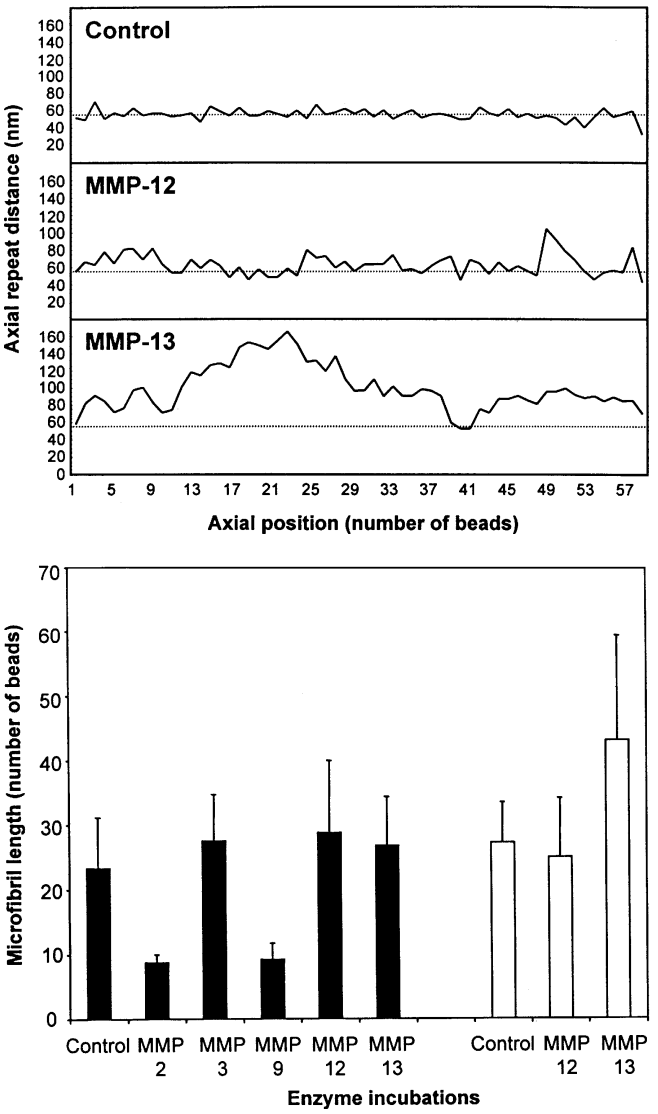

Figure 6 MMP-induced variation in microfibril axial periodicity (top) and length of MMP-treated microfibrils (bottom), as determined by dark field STEM

(**A**) MMP-12 treatment (final concentration 11.0 μg/ml) induced a characteristic microfibril morphology in which regions of normal periodicity were interrupted by regions of extended periodicity. In microfibrils affected by MMP-13 treatment (final concentration 3.2 μg/ml) very few areas of normal periodicity were evident. Dotted line = 55 nm. (**B**) Human zonular microfibrils: 48-year-old (black bars), 68-year-old (white bars). After MMP-2 (final concentration 10.4 μg/ml) and MMP-9 treatment (final concentration 11.6 μg/ml), many short arrays were generated (analysis of variance, $P = 0.067$ and $P = 0.074$ respectively). Long microfibrillar arrays were evident after MMP-12 and MMP-13 treatment. These enzymes appeared to release microfibrils from large aggregated material. Error bars = S.E.M.

further degradation was apparent, including trimming of the ~ 45 kDa product and the appearance of fragments of ~ 34 and 38 kDa (results not shown). nFib-1 appeared to be largely resistant to MMP-3 digestion, although after 20 h a small amount of ~ 45 kDa product was detected (results not shown). MMP-14 rapidly degraded nFib-1 to several fragments (Figure 3A).

Localization of N-terminal cleavage sites

The location of the cleavage site(s) that generated the ~ 45 kDa product was predicted, on the basis of the primary sequence of nFib-1, to occur within either exons 6 and 7 or within exons 10 and 11. Further N-terminal constructs (snFib-1, comprising exons 1–8; proFib-1, comprising exons 9–11) (see Figure 1) were therefore prepared in order to localize the cleavage site. When snFib-1 was incubated for 2 h with the MMPs little degradation was apparent and no major fragments were detected (see Figure 3B). However, proFib-1 was cleaved by all six MMPs, generating products of ~ 9–12 kDa (Figure 3B). These degradation patterns suggest that the cleavage site that generates the ~ 45 kDa product from nFib-1 falls within exons 9–11, which includes the proline-rich region. The corresponding exon 9–11 product of fibrillin-2, glyFib-2, was also cleaved by the MMPs to fragments of ~ 9–12 kDa (Figure 3B), indicating that a similarly located cleavage site exists within fibrillin-2.

Digestion of C-terminal recombinant fibrillin-1 molecules

Labelled recombinant unprocessed cFib-1 was incubated for 15 min, 2 h and 20 h with each of the MMPs to investigate whether these enzymes cleaved these C-terminal regions of fibrillin-1 (Figure 4A). Major fragments (~ 89–95 kDa) were

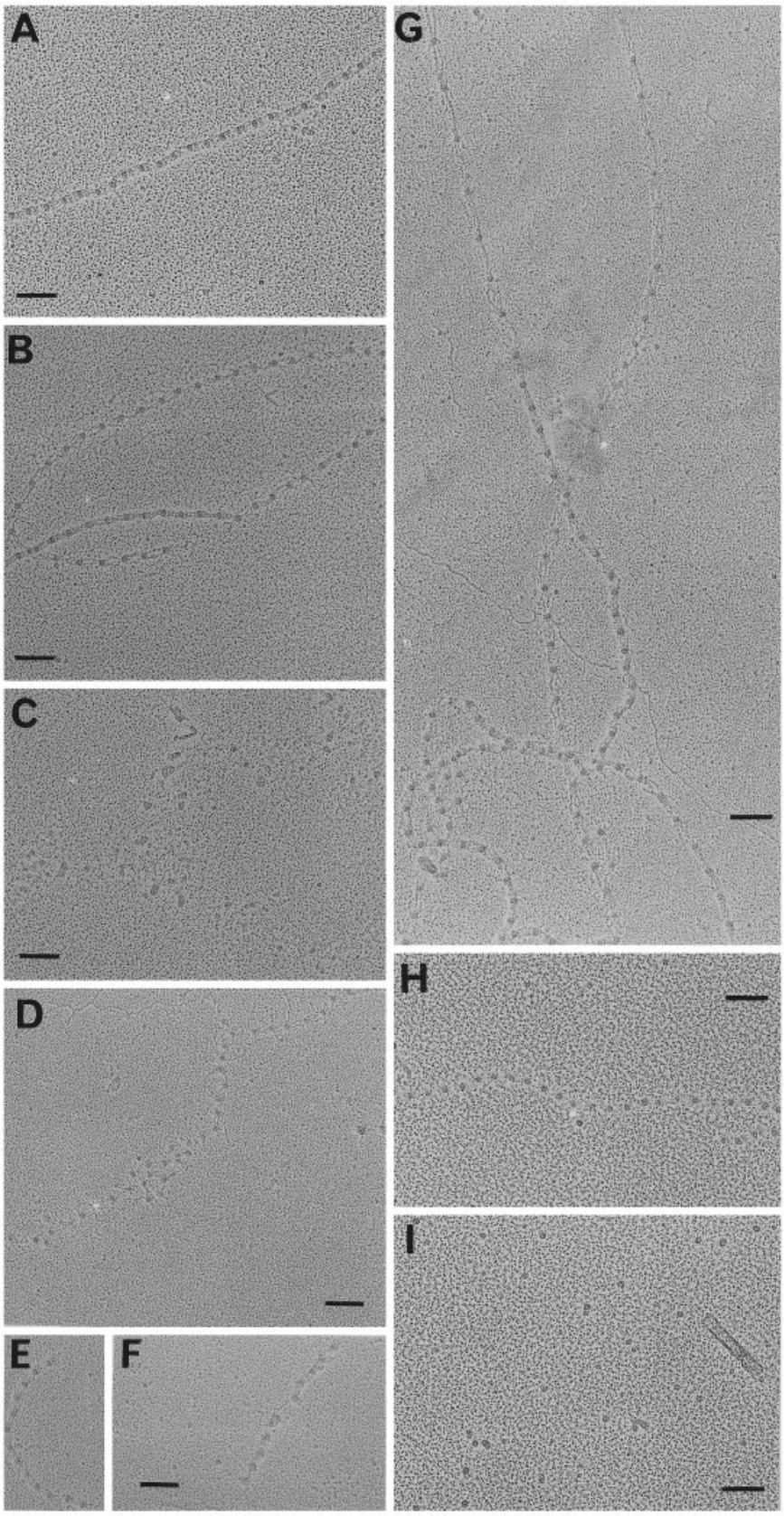

Figure 7 Rotary shadowing electron micrographs of microfibrils isolated from human zonular filaments

detected after 2 h treatment with MMP-2, MMP-12, MMP-13 and MMP-14 (Figure 4A). After 20 h, MMP-3- and MMP-9-treated cFib-1 had undergone some degradation with several fragments apparent (results not shown). scFib-1 was also cleaved by all of the enzymes (except MMP-3), and an abundant fragment of apparent molecular mass ~ 65 kDa was generated (Figure 4A), indicating that a major cleavage site is present within this sequence. In cFib-1 preparations containing unprocessed molecules, plus those processed by furin activity with loss of ~ 0 kDa from the C-terminus, more complex fragmentation patterns and additional fragments in the 20–25 kDa range were apparent (Figure 4B).

Digestion of recombinant normal and mutant cFib-1

In order to determine if amino acid substitutions in cbEGF-like domains affect MMP degradation of fibrillin, site-directed mutagenesis was used to generate mutant fibrillin molecules. Comparison of the fragmentation patterns of normal cFib-1 and a mutant cFib-1 that differed by only a single amino acid (E2447K; cFib-1^{E2447K}) within a cbEGF-like domain (the second of seven contiguous cbEGF-like domains) revealed markedly distinct degradation profiles after incubation with MMP-13, MMP-9, MMP-2 and MMP-12 (Figure 4B). For each enzyme, the MMP-treated cFib-1^{E2447K} contained fragments in common with wild-type cFib-1, but a prominent unique degradation product (~ 47 kDa) was also apparent after MMP-12 and MMP-13 digestions. This mutation, which causes ectopia lentis [41], is predicted to disrupt calcium binding and domain organization. Surprisingly, when a comparable (E2169K) mutation was inserted into the cbEGF-like domain encoded by upstream exon 53 (the second of five contiguous cbEGF-like domains), the MMP fragmentation pattern was indistinguishable from that of the wild-type molecules.

EM analysis of MMP-treated fibrillin-rich microfibrils

Fibrillin molecules form the fibrillar framework of the fibrillin-rich microfibrils, and since MMPs had degraded recombinant fibrillin sequences, apparently accessible within, and crucial to, the integrity of tissue microfibrils, their potential catabolic effects on isolated assembled microfibrils was investigated. When microfibrils from human zonular filaments of two individuals were examined by STEM, before or after overnight incubation at 37 °C with each MMP enzyme at two [E]:[S] ratios, it was clear that these enzymes had affected microfibril organization and integrity (Figures 5 and 6).

After MMP-2 and MMP-9 treatments, increased numbers of short microfibril fragments were detected. In the MMP-12- and MMP-13-treated preparations, many relatively long microfibrils remained. After MMP-12 treatment, a sub-population of microfibrils was identified in which increased bead–bead distances were confined to localized regions (Figure 5; Figure 6, top). After treatment with MMP-13, affected microfibrils exhibited increases in periodicity along their entire length (Figure 5; Figure 6, top). At the higher [E]:[S], many of the MMP-12 and MMP-13 treated microfibrils appeared to have disintegrated.

Untreated and MMP-treated microfibrils were also visualized by rotary shadowing EM in order to examine whether the MMPs had disrupted microfibril organization (Figure 7). In the MMP-12-treated preparations, some extensive microfibrils were detected which in many cases contained disrupted and extended areas (Figure 7B). With increased MMP-12 activity, virtually no intact microfibrils were seen (Figure 7C). MMP-2 and MMP-9 activities resulted in extensive fragmentation of microfibrils (Figures 7D–7F). MMP-13 treated microfibrils were generally similar to those treated with MMP-12, with some extensive microfibrils remaining that had long regions of extended periodicity (Figure 7G). MMP-3 also disrupted microfibrils and in some cases only remnants of beaded domains were observed (Figures 7H and 7I).

DISCUSSION

This study has demonstrated for the first time that members of the MMP family of matrix-degrading enzymes catabolize fibrillin molecules and disrupt fibrillin-rich microfibrils. We have detected major fibrillin-degradation products generated by six different enzymes and have highlighted MMP-specific changes to assembled microfibrils. We have also shown that insertion of a disease-causing mutation (E2447K, a single amino acid substitution within a cbEGF-like domain) [41] markedly alters the pattern of fragmentation. Our studies suggest that MMPs play a key role in the physiological and pathological turnover of fibrillin molecules and microfibrils in the extracellular matrix. Degradation of fibrillin substrates by MMP-2, MMP-3 and MMP-13, which are mainly expressed by stromal cells constitutively or after growth factor induction, suggests that these enzymes may contribute to physiological fibrillin remodelling. MMP-9 and MMP-12 are major products of macrophages and thus may be particularly important in the pathological turnover of fibrillin-rich microfibrils.

The well-established cell-free system supplemented with semi-permeabilized cells very effectively recapitulated secretory pathway folding and other post-translational events [42–45]. The recombinant fibrillin molecules generated in this system contained intra-domain disulphide bonds, as judged by altered electrophoretic mobility on reduction, bound calcium and were N-glycosylated. Fibrillin contains putative tetrabasic furin/PACE (paired basic amino acid converting enzyme) cleavage sites within the unique N- and C-terminal regions, and processing of secreted fibrillin-1 at these sites with removal of ~ 2 kDa and ~ 20 kDa respectively has previously been indicated [17,21]. In the present study we were able experimentally to induce furin-directed processing of cFib-1 by incubating washed cell lysates at 37 °C, and this allowed us to determine whether processing influenced MMP-driven degradation.

Fibrillin-1 is a large glycoprotein which to date has proved difficult to express as a full-length molecule. In this study, we focused on examining MMP-driven proteolysis of extended N- and C-terminal sections of fibrillin-1, which are not only crucial for microfibril assembly and integrity, but also largely accessible within the inter-bead zone of assembled microfibrils [21]. We were particularly interested in investigating whether the unusual proline-rich region, which intersperses cysteine-rich domains and is predicted to be a 'hinge' region, might be a proteolytically susceptible sequence. In a related molecule, LTBP-1, a proline-

Microfibrils were isolated from the zonule of a 38-year-old individual, before and after incubation for 18 h at 37 °C with MMP-2, MMP-3, MMP-9, MMP-12 and MMP-13. (**A**) Uuntreated control. (**B** and **C**) MMP-12 (final concentration 11.0 μg/ml and 27.5 μg/ml respectively). (**D**) MMP-2 (final concentration 10.4 μg/ml). (**E** and **F**) MMP-9 (final concentration 11.6 μg/ml). (**G**) MMP-13 (final concentration 3.2 μg/ml). (**H** and **I**) MMP-3 (final concentration 9.6 μg/ml and 24.0 μg/ml respectively). After MMP-2, MMP-3 and MMP-9 treatments, the microfibrils were largely fragmented. MMP-12 and MMP-13 treatment also disrupted microfibrils; in some fields remaining microfibrillar structures exhibited regions of extended periodicity. Scale bars = 100 nm.

rich linker region undergoes proteolysis with removal of the N-terminus and consequent release of the molecule from matrix storage sites [19]. Moreover, the cFib-1 construct contained long contiguous arrays of cbEGF-like domains interspersed with TB modules similar to those that comprise the remaining central region of the molecule (see Figure 1).

The major ~45 kDa N-terminal fragment identified after digestion of nFib indicated the presence of a major proteolytically susceptible site, and further analysis with snFib-1 and proFib-1 indicated that the cleavage site responsible for removing the entire N-terminal region of the molecule is probably within, or close to, the proline-rich region (exons 9–11). Interestingly, MMP treatment of glyFib-2 (exons 9–11) peptides generated similar-sized degradation fragments to proFib-1, indicating that this corresponding region of fibrillin-2 is also susceptible to cleavage by MMPs and that the N-terminal sequences of both molecules can be removed. Cleavage of unprocessed, processed and truncated forms of the C-terminal region of fibrillin-1 by the MMPs and detection of large degradation products indicates that another major proteolytically susceptible site(s) exists within this sequence. Taking into account the aberrant electrophoretic mobility of the C-terminal fibrillin molecules, which migrated more slowly than expected on the basis of predicted molecular masses possibly due to adoption of an extended rod-like conformation, cleavage is probably within exons 55–57, which would remove the C-terminal sequence. Cleavage at these N- and C-terminal sites could disrupt pericellular microfibril assembly and/or cause gross disruption to pre-assembled microfibrils. Additional MMP cleavage sites may well occur within the central region of the molecule.

Ultrastructural examination revealed complex patterns of disruption to assembled microfibrils after incubation with MMPs. Rotary shadowing highlighted many 'frayed' and fragmented microfibrils, confirming that MMPs disrupt microfibril structure and function. The effects of MMP-12 and MMP-13 digestions appeared complex, with disordered areas of extended periodicity often apparent. It is interesting to speculate that cleavage at the specific N- and/or C-terminal sites identified here may lead to microfibril extension. MMP-induced degradation of microfibril-associated molecules [18–20] may also contribute to microfibril damage.

Removal of calcium from fibrillin-1 molecules and assembled microfibrils has been shown to enhance their degradation by trypsin [16,50]. We have shown here, for the first time, that a disease-causing single amino acid substitution (E2447K) in the second cbEGF-like domain of an array of seven such domains predicted to disrupt calcium binding and domain conformation results in markedly altered electrophoretic mobility and degradation of these mutant fibrillin-1 molecules. In particular, the appearance of a major product of ~47 kDa suggests that conformation changes at or close to the site of the mutation have exposed a cryptic cleavage site. Single amino acid substitutions in cbEGF-like domains are one of the most common mutation types in Marfan syndrome and also cause the fibrillin-2-linked disease congenital contractural arachnodactyly [12,27]. Many of these mutations (and possibly also other mutation types) may cause conformation changes that increase the susceptibility of fibrillin molecules and microfibrils to proteolysis. However, when we prepared another mutant molecule in which effectively the same E → K mutation was inserted within the second cbEGF-like domain (E2169K, exon 53) of the upstream array of five such domains, fragmentation patterns were indistinguishable from the wild-type molecule. Thus mutant domain location within the molecule may have a major impact on molecular conformational changes and susceptibility to degradation; it is also possible that not all cbEGF-like domains contain cryptic MMP cleavage sites. Using Marfan patient dermal fibroblast cultures, we have previously observed many irregular microfibril morphologies and have concluded that such organizational changes may reflect incorporation of defective mutant allele products [51–53]. The present study highlights that altered susceptibility to degradation probably underlies many of these microfibril abnormalities. The results obtained also have major implications for the loss of microfibril and elastic fibre function associated with ageing and physiological remodelling and for interpreting structural microfibrillar defects and genotype–phenotype relationships in Marfan syndrome and related diseases.

J.L.A. is a Wellcome Trust Vision Research Fellow. C.M.K. acknowledges the support of the Medical Research Council. The proFib-1 construct was generated by Sharon Cunliffe. We acknowledge the assistance of the staff of the Corneal Eye Bank Service, Manchester.

REFERENCES

1 Sakai, L. Y., Keene, D. R. and Engvall, E. (1986) J. Cell Biol. **103**, 2499–2509
2 Kielty, C. M. and Shuttleworth, C. A. (1995) Int. J. Biochem. Cell Biol. **2**, 747–760
3 Reber-Muller, S., Spissinger, T., Schuchert, P., Spring, J. and Schmid, V. (1995) Dev. Biol. **169**, 662–674
4 Thurmond, F. A. and Trotter, J. A (1991) J. Expt. Biol. **199**, 1817–1828
5 Mecham, R. P. and Heuser, J. E (1991) in Cell Biology of the Extracellular Matrix (Hay, E. D., ed.), pp. 79–109, Plenum Press, New York and London
6 Keene, D. R., Maddox, K., Kuo, H.-J., Sakai, L. Y. and Glanville, R.W (1991) J. Histochem. Cytochem. **39**, 441–449
7 Kielty, C. M. and Shuttleworth, C. A. (1997) Micros. Res. Tech. **38**, 407–427
8 Maddox, B. K., Sakai, L. Y., Keene, D. R. and Glanville, R. W. (1989) J. Biol. Chem. **264**, 21381–21385
9 Gibson, M. A., Kumaritilake, J. S. and Cleary, E. G. (1989) J. Biol. Chem. **264**, 4590–4595
10 Wright, D. W., McDaniels, C. N., Swasdison, S., Accavitti, M. A., Mayne, P. M. and Mayne, R. (1994) Matrix Biol. **14**, 41–49
11 Pereira, L., Andrikopoulos, K., Tian, J., Lee, S. Y., Keene, D. R., Ono, R., Reinhardt, D. P., Sakai, L. Y., Biery, N. J., Bunton, T. et al. (1997) Nature Genet. **17**, 218–222
12 Ramirez, F. (1996) Curr. Opin. Genet. Dev. **6**, 309–315
13 Corson, G. M., Chalberg, S. L., Dietz, H. C., Charbonneau, N. L. and Sakai, L. Y. (1993) Genomics **17**, 476–484
14 Pereira, L., D'Alessio, M., Ramirez, F., Lynch, J. R., Sykes, B., Pangilinan, T. and Bonadio, J. (1993) Hum. Mol. Genet. **2**, 961–968
15 Cardy, C. M. and Handford, P. A. (1998) J. Mol. Biol. **276**, 855–860
16 Wess, T. J., Purslow, P. P., Sherratt, M. J., Ashworth, J. L., Shuttleworth, C. A. and Kielty, C. M. (1998) J. Cell Biol. **141**, 829–837
17 Milewicz, D. M., Grossfield, J., Cao, S.-N., Kielty, C. M., Covitz, W. and Jewett, T. (1995) J. Clin. Invest. **95**, 2373–2378
18 Brown-Augsburger, P., Broekelmann, T., Mecham, L., Mercer, R., Gibson, M. A., Abrams, W. R., Rosenbloom, J. and Mecham, R. P. (1994) J. Biol. Chem. **269**, 28445–28449
19 Sinha, S., Nevett, C., Shuttleworth, C. A. and Kielty, C. M. (1998) Matrix Biol. **17**, 529–545
20 Reinhardt, D. P., Sasaki, T., Dzamba, B. J., Keene, D. R., Chu, M. L., Gohring, W., Timpl, R. and Sakai, L. Y. (1996) J. Biol. Chem. **271**, 19489–19496
21 Reinhardt, D. P., Keene, D. R., Corson, G. M., Poschl, E., Bachinger, H. P., Gambee, J. E. and Sakai, L. Y. (1996) J. Mol. Biol. **258**, 104–116
22 Liu, W., Qian, C., Comeau, K., Brenn, T., Furthmayr, H. and Franke, U. (1996) Hum. Mol. Genet. **5**, 1581–1587
23 Qian, R. Q. and Glanville, R. W. (1997) Biochemistry **36**, 15841–15847
24 Zugibe, F. T. and Brown, K. D. (1960) Circ. Res. **8**, 287–295
25 Nejjar, I., Pieraggi, M. T., Thiers, J. C. and Bouissou, H. (1990) Atherosclerosis **80**, 199–208
26 Pasquali-Ronchetti, I., Baccarani-Contri, M., Fornieri, C., Mori, G. and Quaglino, D. (1995) Micron **24**, 75–89
27 Dietz, H. C. and Pyeritz, R. E. (1995) Hum. Mol. Genet. **4**, 1799–1809
28 Chambers, A. F. and Matrisian, L. M. (1997) J. Natl. Cancer Inst. **89**, 1260–1270
29 Reynolds, J. J. and Meikle, M.C. (1997) Peridontol. 2000 **14**, 144–157
30 Brown, D., Hamdi, H., Bahri, S. and Kenney, M. C. (1994) Curr. Eye Res. **13**, 639–647
31 Guggenheim, J. A. and McBrien, N. A. (1996) Invest. Ophthalmol. Visual Sci. **37**, 1380–1395

32 De La Paz, M. A., Itoh, Y., Toth, C. A. and Nagase, H. (1998) Invest. Ophthalmol. Visual Sci. **39**, 1256–1260
33 Plantner, J. J., Smine, A. and Quinn, T. A. (1998) Curr. Eye Res. **17**, 132–140
34 Ando, H., Twinning, S. S., Yue, B. Y. J. T., Zhou, X., Fini, M. E., Kaiya, T., Higginbotham, E. J. and Sugar, J. (1993) Invest. Ophthalmol. Visual Sci. **34**, 3541–3548
35 Kielty, C. M., Woolley, D. E., Whittaker, S. P. and Shuttleworth, C. A. (1994) FEBS Lett. **351**, 85–89
36 Koklitis, P. A., Murphy, G., Sutton, C. and Angal, S. (1991) Biochem. J. **276**, 217–221
37 Murphy, G., Willenbrock, F., Ward, R. V., Cockett, M. I., Eaton, D. and Docherty, A. J. P. (1992) Biochem. J. **283**, 637–641
38 Knäuper, V., López-Otin, C., Smith, B., Knight, G. and Murphy, G. (1996) J. Biol. Chem. **271**, 1544–1550
39 Jeng, A. Y., Wong, M., Duelfer, T., Shapiro, S. D., Kramer, R. A. and Hu-Si, N. A. (1995) J. Biochem. **117**, 216–221
40 Gronski, T. J., Martin, R. L., Kobayashi, D. K., Walsh, B. C., Holman, M. C., Huber, M., Van Wart, H. E. and Shapiro, S. D. (1997) J. Biol. Chem. **272**, 12189–12194
41 Kainulainen, K., Karttunen, L., Puhakka, L., Sakai, L. and Peltonen, L. (1994) Nature Genet. **6**, 64–69
42 Wilson, R., Allen, A. J., Oliver, J., Brookman, J. L., High, S. and Bulleid, N. J. (1995) Biochem. J. **307**, 679–687
43 Lees, J. F., Tasab, M. and Bulleid, N. J. (1997) EMBO J. **16**, 908–916
44 Illidge, C., Kielty, C. M. and Shuttleworth, C. A. (1998) J. Biol. Chem. **273**, 22091–22095
45 McLaughlin, S. H. and Bulleid, N. J. (1998) Biochem. J. **331**, 793–800
46 Kielty, C. M., Cummings, C., Whittaker, S. P., Shuttleworth, C. A. and Grant, M. E. (1991) J. Cell Sci. **99**, 797–807
47 Kielty, C. M., Hanssen, E. and Shuttleworth, C. A. (1998) Anal. Biochem. **255**, 108–122
48 Sherratt, M. J., Holmes, D. F., Shuttleworth, C. A. and Kielty, C. M. (1997) Int. J. Biochem. Cell Biol. **29**, 1063–1070
49 Nakayama, K. (1997) Biochem. J. **327**, 625–635
50 Reinhardt, D. P., Ono, R. N. and Sakai, L. Y. (1997) J. Biol. Chem. **272**, 1231–1236
51 Kielty, C. M., Raghunath, M., Siracusa, L. D., Sherratt, M. J., Peters, R., Shuttleworth, C. A. and Jimenez, S. J. (1998) J. Cell Biol. **140**, 1159–1166
52 Kielty, C. M. and Shuttleworth, C. A. (1994) J. Cell Biol. **124**, 997–1004
53 Kielty, C. M., Phillips, J. E., Child, A. H., Pope, F. M. and Shuttleworth, C. A. (1994) Matrix Biol. **14**, 191–199

Received 27 October 1998/9 February 1999; accepted 4 March 1999